

EXPERIMENTAL STUDY OF JET FLOW FIELD BY DUAL HOLOGRAM INTERFEROMETRY

Peng Lv*, Zhimin Chen, Xing Wang

*Northwestern Polytechnical University, Xian, Shaanxi, 710072, China

Keywords: gas dynamotor, jet flow, density, dual hologram interferometry

Abstract

The research on the density distribution of jet flow field is beneficial to the shape design of the projectile fuse gas dynamotor. Dual hologram interferometry is involved to obtain the interferometry picture of jet flow field with the model of gas dynamotor at M (Mach number) $=0.6$. The paper tries to provide a new method to analyze the holographic interferometry picture, aiming to find out the density distribution of the jet flow field around the gas dynamotor model. Finally, the study proves that the experimental result is believable, through comparing with the numerical simulation result of density distribution of the jet flow field around the model, which is based on S - A turbulence model for numerical integration of $2D$ N - S equations and structured grids with H type.

1 Introduction

Jet flow is a special flow which indicates that fluid spurts out from all kinds of nozzles. It is not restricted by solid boundaries, and freely diffuses in a space. Because of the differences between jet flow and ordinary wind tunnels flow, many scholars have been researching the projectile fuse gas dynamotor by the jet facility.

The gas dynamotor, working as the power source of projectile, provides triggering signal, so the shape design of the gas dynamotor is significant for a successful projectile. Proved by a number of experiments, jet facility can authentically simulate the working condition of the projectile flying in the atmosphere [1]. However, the density of atmosphere received by

the gas dynamotor will be changed along with the change of the height and velocity of the authentic flight. It is necessary to utilize the experimental data of density distribution to revise the result of telemetry density distribution of atmosphere. Therefore, it is challenging for the projectile designers to measure the density distribution of jet flow field around the gas dynamotor. So far, there has not been an acceptable and feasible method regarding this.

In the present paper, firstly, dual hologram interferometry is involved to obtain the holographic interferometry picture of jet flow field around the gas dynamotor model at $M=0.6$. Secondly, the relative light intensity method is employed to analyze the holographic interferometry picture, aiming at finding out the density distribution of the jet flow field around the model. Finally, the experimental result is investigated by comparing with the numerical simulation result of density distribution of the jet flow field around the model, which is based on S - A turbulence model for numerical integration of $2D$ N - S equations and structured grids with H type. The research proves that the combination of dual hologram interferometry and numerical simulation is effective to obtain the density distribution of the jet flow field around the gas dynamotor model quantitatively, which will be significant to research more complicated flow field in the future.

2 Principles

To make a holographic dry plate exposed twice in the process of dual hologram interferometry recording, the first exposure of the jet flow field is without the gas dynamotor model, and the

holographic dry plate can record the light amplitude and the light phase without disturbance. The second exposure of the jet flow field is with the model, and the same holographic dry plate can record the light amplitude and the light phase with disturbance. The changes of the light path and the light phase are caused by the density change of the jet flow field. So, the holographic dry plate will record the holographic interferometry stripes [2, 3, 4, 5].

The light at the time of first exposure is

$$o_1 = A_0 \exp(-i\phi_0) \quad (1)$$

The light at the time of second exposure is

$$o_2 = A_0 \exp[-i(\phi_0 + \Delta\phi)] \quad (2)$$

If the two exposure times are equal, the holographic interferometry picture with largest contrast will be recorded on the holographic dry plate. So, the light intensity distribution of the holographic interferometry picture is

$$I = 2\beta^2 A_r^4 A_o^2 \tau^2 [1 + \cos(\Delta\phi)] \quad (3)$$

Where β is the sensitivity of the hologram, A_o and A_r are the actual amplitude of the object light and the reference light in the recorded plane respectively, τ is the exposure time. The shape of holographic interferometry stripes completely depends on the of the phase function $\Delta\phi(x, y)$.

The relationship of relative light intensity and light phase is

$$I_r = \frac{255}{2} [1 + \cos(\Delta\phi_m)] \quad (4)$$

Then

$$\Delta\phi_m = 2m\pi - \arccos\left(\frac{2I_r}{255} - 1\right) \quad (5)$$

($m = 0, \pm 1, \pm 2, \pm 3 \dots$)

When $\Delta\phi$ is equal to $2m\pi$, the light intensity will reach the maximum value $4\beta^2 A_r^4 A_o^2 \tau^2$, which displays the bright stripes while when $\Delta\phi$ is equal to $(2m+1)\pi$, the light intensity will reach the minimum value 0, which displays the dark stripes.

So, the light phase change is a direct reflection of the holographic interferometry stripes. The relationship of the light phase change and refractive index of the jet flow field is

$$\Delta\phi = \frac{2\pi}{\lambda} \int_0^L [n(x, y, z) - n_0] dz \quad (6)$$

Where λ is the laser wave length, L is the test length, n_0 is the initial refractive index of the jet flow field without disturbance, $n(x, y, z)$ is the refractive index of the disturbed jet flow field. Combine with *Gladstone-Dale* formula

$$n = K\rho + 1 \quad (7)$$

Then

$$\Delta\phi = \frac{2\pi L K \Delta\rho}{\lambda} \quad (8)$$

Where K is the *Gladstone-Dale* constant ($K = 0.00025 \text{ m}^3/\text{kg}$). We can calculate the density of the jet flow field according to the phase information from holographic interferometry stripes [6, 7, 8].

3 Experiment Equipments

3.1 Dual hologram interferometry optical system

In figure 1, *RL* is a ruby laser; M_1, M_2, M_3, M_4 are the turn-reflect mirrors; M_5, M_7 are the schlieren mirrors; M_6 is the schlieren-reflect mirror; L_1, L_3 are expanding beam lenses; L_2 is the collimation lens; *SP* is the adjustable splitter; *H* is holographic plane.

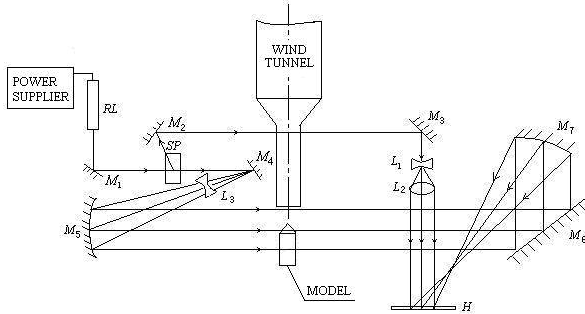


Fig. 1. The diagram of dual hologram interferometry optical system

3.2 Jet facility

This experiment was conducted at Fluid Mechanics Research Laboratory, Northwestern Polytechnical University [9]. The jet facility was designed to obtain the subsonic jet flow field to study aerodynamic characteristics of the projectile fuse gas dynamotor. The air supply system for the jet flow is provided from a high-pressure storage tank coupled to a high displacement air compressor. It is shown in figure 2.



Fig. 2. Authentic picture of the jet facility

The details of the jet facility are shown in figure 3.

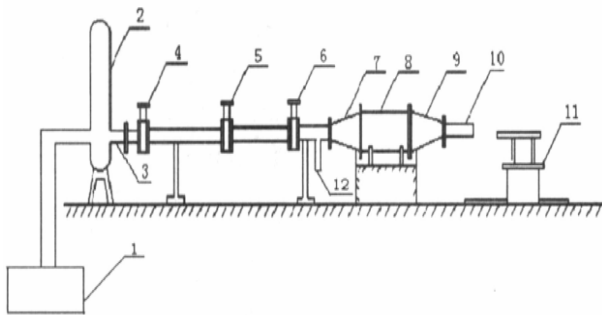


Fig. 3. Details of the jet facility

1. Air compressor
2. Storage tank
3. Coupled pipe
4. Tight valve
5. Pressure regulator valve
6. Fast valve
7. Diffuser section
8. Steady flow section
9. Contraction section
10. Jet pipe
11. Fixed model device
12. Other nozzle interface

3.3 Ruby laser

Laser model is TD-05 Q-switched pulse ruby laser. Laser wavelength is 694.3nm; Single pulse energy is 1J, double-pulse energy is 0.5J; Double pulse interval is 100-700 μs with the minimum adjustable step is 1 μs; Pulse width is about 50ns; Coherence length is greater than 1.5m.

4 Experimental Data Analysis

The model of the projectile fuse gas dynamotor is applied in this experiment. The experimental condition: attack angle $\alpha = 0^\circ$; Mach number $M=0.6$.

Figure 4 shows the experimental result of jet flow field with the gas dynamotor model. From the figure, the density distribution of the jet flow field around the gas dynamotor model is approximately symmetrical. The dark stripes can be regarded as the equal density line. According to the distance between bright and dark stripes in the figure, the relative density changes can be obtained but the density. This paper provides a new method to analyze the holographic interferometry picture by relative light intensity.



Fig. 4. The holographic interferometry picture

According to relative light intensity formula

$$I_r = \frac{255 I}{I_{max}} \quad (9)$$

Where I is the light intensity of the holographic interferometry picture, I_{max} is the maximum value of the light intensity in the picture.

As shown in Figure 5, the light intensity distribution of the holographic interferometry picture was converted to the relative light intensity distribution. Axis X and axis Y indicate the number of the picture pixels while axis Z indicates the relative light intensity.

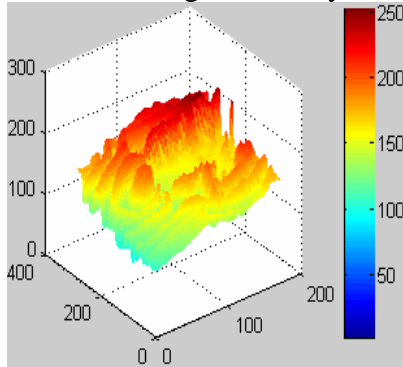


Fig. 5. The relative light intensity distribution

According to the peaks of the light intensity, five levels were classified in the holographic interferometry picture. They are the zero level stripe, the first level stripe, the second level stripe, the third level stripe, the fourth level stripe in order, as is shown in Figure 6.

Considering that the density of far field is a constant, so the zero level stripe is regarded as a standard stripe. Figure 7 shows the relative light intensity distribution of each level stripe. Where Axis X and axis Y indicate the pixels number of each level stripe, axis Z indicates the relative light intensity of each level stripe. According to the formula about the relative light intensity and the light phase change

$$\Delta\phi_m = 2m\pi - \arccos\left(\frac{2I_r}{255} - 1\right) \quad (10)$$

($m=1, 2, 3, 4$)

Figure 8 shows the phase difference between every level stripe and zero level stripe. Axis X and axis Y indicate the pixels number of each level stripe, axis Z indicates the phase difference. Also

$$\Delta\phi_m = \frac{2\pi LK(\rho_m - \rho_0)}{\lambda} \quad (11)$$

Where ρ_0 is 1.225 kg/m^3 . So, the density distribution of the jet flow field around the projectile fuse gas dynamotor model can be described, as is shown in Figure 9.

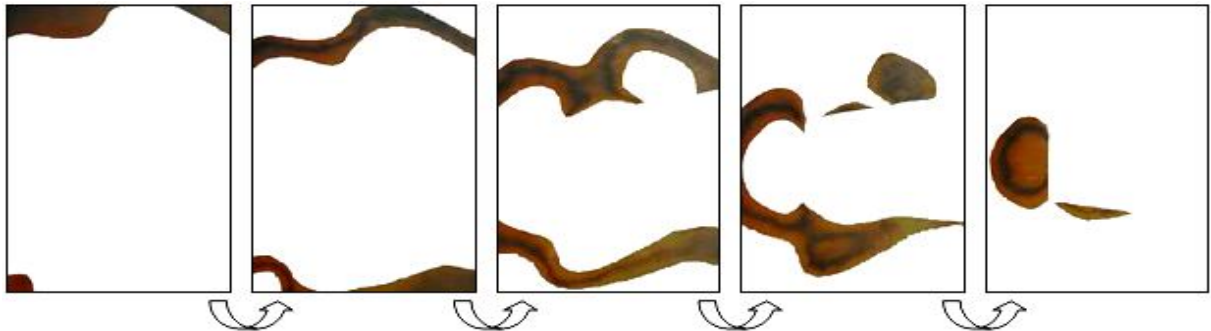


Fig. 6. The classified stripes

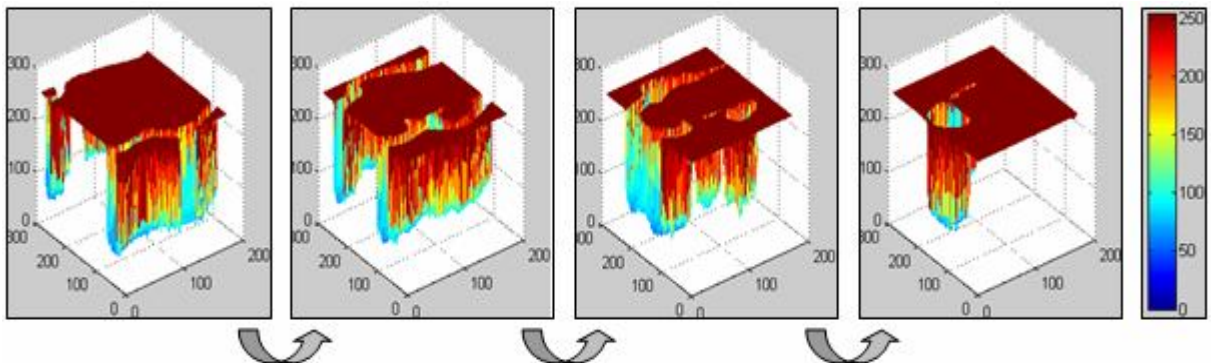


Fig. 7. The relative light intensity distribution

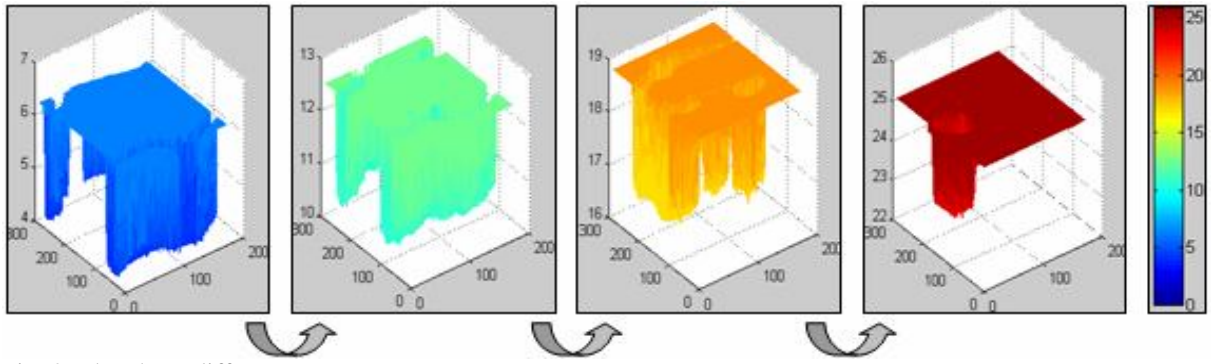


Fig. 8. The phase difference

From the picture, the density variations of the jet flow field around the model are not very extreme. The density of the stagnation point front of the model is maximum value, and the density decreases gradually from the stagnation point to the flow field which is around it.

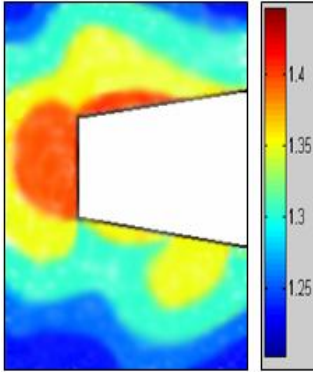


Fig. 9. The density distribution of the jet flow field

5 Numerical simulation

5.1 Flow Solver

The 2D compressible *N-S* equations can be described

$$\frac{\partial U}{\partial t} + \frac{\partial F}{\partial x} + \frac{\partial G}{\partial y} = \frac{\partial V_1}{\partial x} + \frac{\partial V_2}{\partial x} + \frac{\partial W_1}{\partial y} + \frac{\partial W_2}{\partial y} \quad (12)$$

Where *U* is the vector of conserved variables and *F*, *G*, *V* and *W* are flux vectors.

The solution algorithm to compute the *N-S* equations is based on the finite volume. And the *S-A* turbulence model was employed which is suitable for simulating both interior and exterior flow in a moderate complexity, and boundary flow under the pressure grads.

5.2 Grids and boundary settings

With the merits of body-fit structured mesh in viscous computation, *H* grid is applied to create structured grids of the computation area around the model. Figure 10 shows the computational grids.

Stagnation pressure *p*₀ was measured by pitot-static probe arranged in the steady flow section of the jet facility. And static pressure *p* was measured by pitot-static probe arranged at the outlet of the jet facility [10].

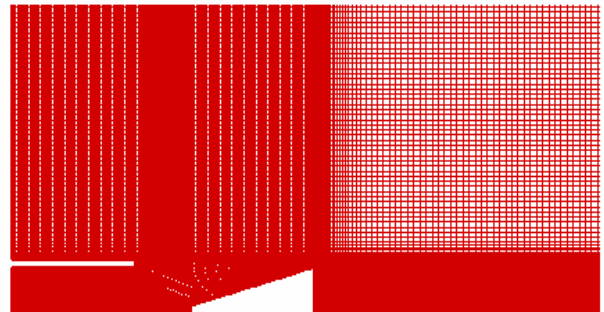


Fig. 10. The computational grids

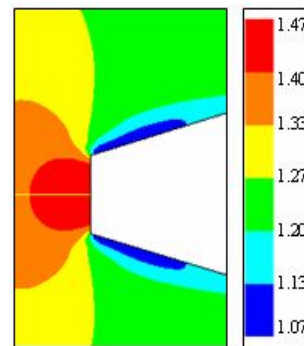


Fig. 11. The numerical simulation result

The numerical simulation result is shown in Figure 11.

5.3 Summary

5.3.1 Characteristics

The same characteristics: The density of the stagnation point possesses maximum value, and the density decreases gradually from the stagnation point to the surrounding flow field.

The different characteristics: The density of two sides of the gas dynamotor model surface is equal to the density of the stagnation point approximately in the experimental result. But the density of two sides of the model surface is far less than the density of the stagnation point.

3.3.2 Data

Figure 12 shows the comparison of the density distribution from the experimental result and the numerical simulation result at the distance of 10mm front the model. Axis X indicates the relative length of the jet flow field and axis Y indicates the density distribution.

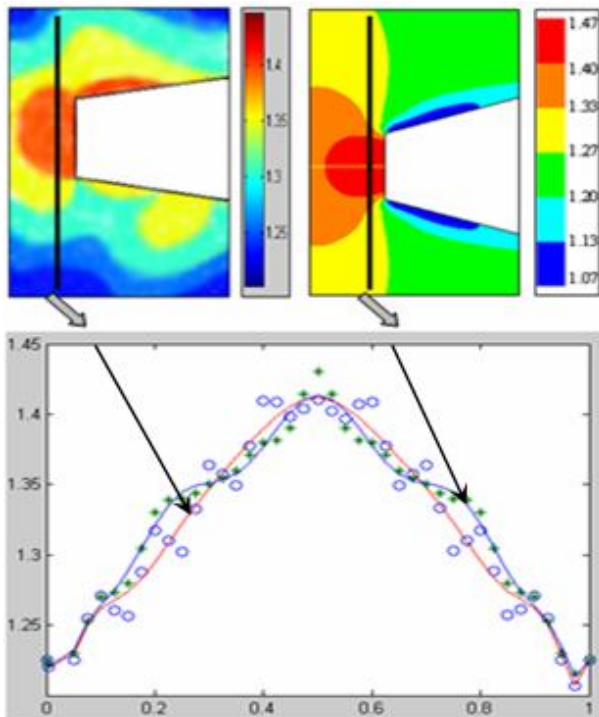


Fig. 12. The comparison of the density distribution (Red line with o indicates the experimental result. Blue line with * indicates the numerical simulation result.)

These discrepancies may be caused by the model size error or the fixed model angle error.

6 Conclusion

The relative light intensity method is provided here to analyze the holographic interferometry picture taken by dual hologram interferometry, in order to gain the density distribution of the jet flow field around the model of gas dynamotor of projectile fuse by classifying the holographic interferometry picture level-by-level. The experimental result based on the method is believable through comparing it with the numerical simulation result. The combination of dual hologram interferometry and numerical simulation is effective to measure the density distribution of the jet flow field around the gas dynamotor model.

References

- [1] Zhimin C, Kunlong Y. Studies on experimental equipments and testing technology of gas dynamotor. *Journal of Experimental Mechanics*, Vol. 19, No. 3, pp 386-390, 2004.
- [2] Andrew C and Tom P. Acoustic beam forming and holography measurements of modified boundary layer trailing-edge Noise. *12th AIAA/CEAS Aero Acoustics Conference*, Massachusetts, Vol. 2566, 2006-2566, pp 1-14, 2006.
- [3] W Spring. Conversion of standard schlieren system to holography in the navy's hypervelocity wind tunnel. *18th AIAA Aerospace Ground Conference*, Colorado, Vol. 2648, 94-1648, pp 1-10, 1994.
- [4] Qinzhong S. Structural optimization based on holographic neural network and its extrapolation. *1998 AIAA Conference*, Missouri, Vol. 4975, 98-4975, pp 2124-2132, 1998.
- [5] Radley R J Jr, Havener A G. The application of dual hologram interferometry to wind tunnel testing. *AIAA Journal*, vol. 11, No. 9, pp 1332-1333, 1973.
- [6] Jiangang W, Xinghua M, Guozhi W. Two-exposure holography for study of shockwave flow generated by a model in a supersonic wind channel. *Acta Photonica Sinica*, Vol. 26, No. 4, pp 373-378, 1997.
- [7] Jiechuan F. Latter-day flow visualization technology. 1st edition, *National defense industry press*, 2002.
- [8] Merzkirch W. Flow Visualization. 1st edition, *Science press*, 1991.
- [9] Zhimin C, Hailong W, Muliang Y. Measuring the Density Distribution of Flow Field in Jet Facility by Laser Dual Hologram Interferometry. *Applied Laser*, Vol. 27, No. 3, pp 201-204, 2007.
- [10] Weigang Y, Zhimin C, Zhenyi L. Effects of warhead model dimension on two-dimensional supersonic jet field. *Journal of Propulsion Technology*, Vol. 27, No. 4, pp 336-338, 2006.

Copyright Statement

The authors confirm that they, and/or their company or organization, hold copyright on all of the original material included in this paper. The authors also confirm that they have obtained permission, from the copyright holder of any third party material included in this paper, to publish it as part of their paper. The authors confirm that they give permission, or have obtained permission from the copyright holder of this paper, for the publication and distribution of this paper as part of the ICAS2010 proceedings or as individual off-prints from the proceedings.